




Tracheid buckling buys time, foliar water uptake pays it back: Coordination of leaf structure and function in tall redwood trees

Alana R. O. Chin¹  | Paula Guzmán-Delgado¹  | Stephen C. Sillett² |
Lucy P. Kerhoulas² | Anthony R. Ambrose³ | Andrew R. McElrone⁴  |
Maciej A. Zwieniecki¹

¹Department of Plant Sciences, University of California Davis, Davis, California, USA

²Department of Forestry and Wildland Resources, Humboldt State University, Arcata, California, USA

³Department of Integrative Biology, University of California Berkeley, Berkeley, California, USA

⁴USDA-ARS & Viticulture and Enology Department, University of California Davis, Davis, California, USA

Correspondence

Alana R. O. Chin, Plant Sciences Department, University of California Davis, Davis CA, 95616, USA.

Email: alanaroseo@gmail.com

Present addresses

Alana R. O. Chin, Department of Atmosphere and Climate Science (D-USYS), AROC: Institute for Integrative Biology, ETH, Zürich, Switzerland.

Anthony R. Ambrose, The Marmot Society, South Lake Tahoe, California, USA.

Abstract

Tracheid buckling may protect leaves in the dynamic environments of forest canopies, where rapid intensifications of evaporative demand, such as those brought on by changes in light availability, can result in sudden increases in transpiration rate. While treetop leaves function in reliably direct light, leaves below the upper crown must tolerate rapid, thermally driven increases in evaporative demand. Using synchrotron-based X-ray microtomography, we visualized impacts of experimentally induced water stress and subsequent fogging on living cells in redwood leaves, adding ecological and functional context through crown-wide explorations of variation in leaf physiology and microclimate. Under drought, leaf transfusion tracheids buckle, releasing water that supplies sufficient temporal reserves for leaves to reduce stomatal conductance safely while stopping the further rise of tension. Tracheid buckling fraction decreases with height and is closely coordinated with transfusion tissue capacity and stomatal conductance to provide temporal reserves optimized for local variation in microclimate. Foliar water uptake fully restores collapsed and air-filled transfusion tracheids in leaves on excised shoots, suggesting that trees may use aerial water sources for recovery. In the intensely variable deep-crown environment, foliar water uptake can allow for repetitive cycles of tracheid buckling and unbuckling, protecting the tree from damaging levels of hydraulic tension and supporting leaf survival.

KEYWORDS

embolism repair, foliar water uptake, microclimate, *Sequoia*, tracheid buckling, transfusion tissue

This is an open access article under the terms of the Creative Commons Attribution-NonCommercial-NoDerivs License, which permits use and distribution in any medium, provided the original work is properly cited, the use is non-commercial and no modifications or adaptations are made.

© 2022 The Authors. *Plant, Cell & Environment* published by John Wiley & Sons Ltd.

1 | INTRODUCTION

Treetop leaves grow under consistently bright conditions, but little is known about the extent of microclimatic variability or physiological responses to abrupt changes below the treetops in tall forest trees. For example, sunflecks, shafts of direct light that deeply penetrate the canopy, can increase leaf temperatures by as much as 20°C in 1 min (Schymanski et al., 2013). Such a temperature fluctuation can raise the vapor pressure deficit (VPD) by approximately 2 kPa, increasing transpirational demand (ΔE). The hydraulic supply needed to sustain ΔE during rapid VPD shifts may generate excessive tension, inducing damage to the hydraulic path within leaves if stomatal conductance (g_s) does not decrease. The time required to close stomata is biologically significant. For example, in *Metasequoia glyptostroboides* (Hu and W.C. Cheng), stomatal stabilization requires approximately 400 s following a +2 kPa vapor pressure deficit increase (ΔVPD), a value consistent with other conifers (Martins et al., 2016; McAdam & Brodribb, 2014). Relatively slow stomatal response puts leaves at risk for a sudden increase in hydraulic tension if sunflecks, or other intense perturbations, are not met with locally available water reserves sufficient to cover ΔE while stomata close to an aperture that will allow the leaf to survive at higher VPD. Insufficient local hydraulic reserves might endanger key structures if tension, translated down the hydraulic path, causes embolism in woody xylem.

Conifer leaves can lose 5%–20% of their water content before losing turgor, possibly because they possess a relatively high-capacity mid-vein consisting mostly of water-filled tracheid cells (Bannister, 1986; Esau, 1977). Under water stress, groups of tracheids flanking the xylem, collectively called transfusion tissue (Esau, 1977; Figure 1a), can buckle (Azuma et al., 2016; Brodribb & Holbrook, 2005; Parker, 1952; Zhang et al., 2014), decreasing their volume. Transfusion tracheid buckling may provide water that can be used to sustain a sudden increase in evaporative demand, until stomata close, perhaps explaining why transfusion tissue volume increases with height in multiple species (Azuma et al., 2016; Chin & Sillett, 2019; Oldham et al., 2010). However, transfusion tracheid buckling can be followed by cavitation and

formation of embolisms (Tyree & Sperry, 1989), and if not refilled, buckling-based hydraulic protection would work only once. Deep crowns of tall redwoods (*Sequoia sempervirens* (D. Don) Endl.) can support >80m of vertically continuous foliage, reaching from shady depths with <10% light availability to emerge above the canopy in open sky (Oldham et al., 2010; Sillett & Van Pelt, 2007). Like most trees, *Sequoia* is capable of absorbing water across the surface of its leaves, possibly explaining how accumulated damage is repaired (Broderson & McElrone, 2013; Burgess & Dawson, 2004; Schreel & Steppe, 2020). Does tracheid buckling protect leaves, and can foliar water uptake enable them to recover?

Our objectives are to assess leaf tracheid buckling and examine the role of foliar water uptake in stress recovery by exposing experimentally bench-dried leaves to dense fog. We hypothesize that transfusion tracheid buckling releases a quantity of water sufficient to meet transient increases in transpirational demand, allowing for typical time delays in stomatal closure and providing a mechanism to stop temporarily the translation of tension. Furthermore, foliar absorption of water not only reduces xylem stress in tall conifers but also permits refilling of collapsed tracheids necessary for cyclic protection during multi-year leaf lifespans. We visualize the impacts of experimental drought and leaf wetting with synchrotron-based X-ray microtomography and explore the structural, physiological, and ecological context of our experimental results to assess the impact of cellular buckling across the full range of potential conditions. Physiological, anatomical, and climatic investigations spanning the height-gradient reveal the ways in which leaves respond to environmental signals and are crucial to understanding tree function.

2 | MATERIALS AND METHODS

2.1 | Experimental drought and exposure to fog

To extend the applicability of our results across the geographic range of *Sequoia*, we collected nine small samples (shoot clusters, ~1 cm

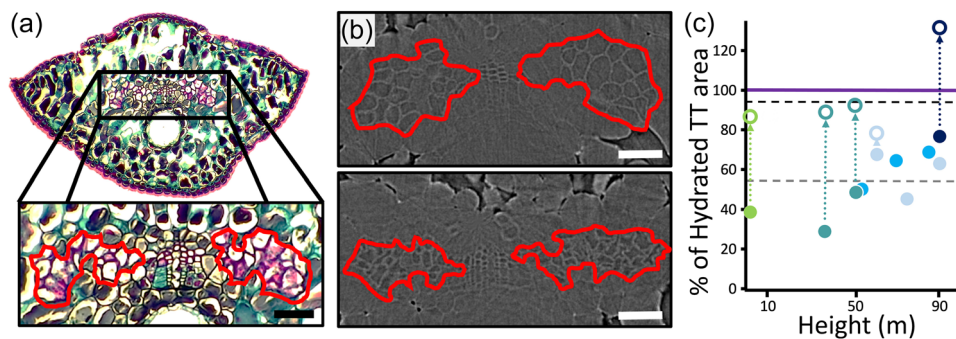


FIGURE 1 Transfusion tissue structure and buckling. (a) The water-filled transfusion tissue (TT) of redwood leaves, outlined here in red, appears on either side of the vascular bundle in a representative leaf from 90 m. (b) MicroCT scans of 90-m-high leaves: top panel shows round tracheids in TT of fully hydrated leaf, and bottom panel shows buckled tracheids in the TT of an experimentally droughted leaf from the same sample. (c) Percent of TT area change compared to their paired-hydrated leaf (purple line at 100%), closed circles = dried treatment, and open circles = fogged leaves. Colors represent individual trees, dashed arrows indicate the fog recovery within shoot clusters. Grey dashed line represents mean dried TT area (55% of hydrated), black line represents mean fog-recovered TT area (95% of hydrated). Scale bars = 0.05 mm.

TABLE 1 Experimental design. Individual shoot clusters from five trees were divided and exposed to three treatments (see Figure 2)

Tree	Tree height (m)	Shoot cluster	Sample height (m)	Treatments		
				Hydrated	Dried	Fogged
1	18	1A	2	X	X	X
2	97	2A	37	X	X	X
		2B	51	X	X	X
3	98	3A	90	X	X	X
4	101	4A	61	X	X	X
		4B	75	X	X	
		4C	90	X	X	
5	103	5A	54	X	X	
		5B	70	X	X	
		5C	85	X	X	

Note: Bold Xs indicate samples with a replicate leaf.

basal diameter) from four tall trees in three locations. Two samples were collected at 37 and 51 m from a 97-m-tall tree in Richardson Redwood Reserve, a third sample was collected at 90 m from a 98-m-tall tree in Jedediah Smith Redwoods State Park, and six samples were collected from a 101-m-tall tree (at 61, 75, and 90 m) and a 103-m-tall tree (at 54, 70, and 85 m) growing in Hedy Woods State Park (all in California, Table 1). All samples came from closed-canopy forests with natural gradients in light availability. We sampled across the vertical gradient to quantify height-associated trends in tracheid buckling and how this might relate to local hydraulic risk. Finally, to confirm that tracheid buckling is widespread in *Sequoia* and not restricted to tall trees, a tenth verification sample was collected at 2 m from an 18-m-tall isolated tree grown in a hot site outside the species' native range on the UC Davis campus. Although redwood leaves do not strongly acclimate to their light environment in comparison to other conifers (Oldham et al., 2010), we assume that there may be unrecognized differences between in-range and out-of-range leaves and between short and tall trees, hence this tenth sample was excluded from analyses of height-based buckling fraction.

All 10 sample shoot-clusters (9 tall and 1 verification) were recut under water and allowed to rehydrate through their cut stem ends for at least 48 h (hydrated control class, $N = 10$, all water potentials ≥ -0.01 MPa) before sub-sampling for experimental treatments (Figure 2, Table 1). The first subsample (hydrated class) was then carefully removed from each of the 10 larger samples by cutting in melted paraffin ($\sim 50^\circ\text{C}$) to form a seal over the woody cut surfaces on both sample and subsample, without exposing the leaf material to wax (Chin & Sillett, 2016). The sealed subsamples were then bench dried to just before their estimated turgor loss points (from Ishii et al., 2014), a water potential (Ψ) range of -1.9 to -2.1 MPa (dried class, $N = 10$). During dry-down we periodically removed individual leafy shoots from each sample to monitor the

Ψ decrease with a pressure chamber. Upon reaching the target Ψ , the second subsample was removed (Dried Class) and placed in sealed, dark plastic bags containing small pieces of wet tissue paper (not contacting the sample) and refrigerated ($\sim 4^\circ\text{C}$) to prevent further water loss. Finally, the third subsample was removed from half of the bench-dried branches, sealed with paraffin as above, exposed to a 7 h fogging event (following the method in Guzmán-Delgado et al., 2018), and then placed in a sealed bag for 18–26 h (fogged class, $N = 5$, all $\Psi \geq -0.01$ MPa, samples from 2, 37, 51, 61, and 90 m, Table 1). The intention of this latter treatment was to mimic natural conditions where leaves were exposed to atmospheric moisture and then remained wet for an extended period of time.

We selected a peripheral leaf from each subsample (from the original 10 shoot clusters) in the hydrated, dried, and fogged treatment classes (10 shoots \times 3 treatments: $N = 10$ hydrated, + 10 dried, + 5 fogged = 25 samples, Table 1). We were able to scan replicate-pairs of leaves from 4 of the 10 shoots (25 samples, plus 4 replicate leaves \times 3 treatments = 37 leaf scans, see Table 1). Due to time constraints on microCT use, we could not scan replicates for all shoots, but we were able to disperse replication among the three treatment classes, and mean values were later used for replicates (Table 1). Selected leaves were scanned using synchrotron-based high-resolution X-ray computed tomography (microCT) at the Advanced Light Source (beamline 8.3.2, Lawrence Berkeley National Labs).

Leaves were detached from the shoot and placed in a pipette tip into which we breathed moist air before sealing with Parafilm to prevent further water loss. Leaves were scanned once only to avoid any potential impacts on active portions of drought and recovery processes that may be reliant on RNA synthesis (Petruzzellis et al., 2018). Segments were scanned at 15 keV in the synchrotron X-ray beam while being rotated through 0 – 180° in increments of 0.25° . After each incremental rotation, the X-ray image was magnified through a series of lenses and relayed onto a 4 megapixel charge coupled device camera yielding approximately 1500, two-dimensional tomographic projections per sample that were then reconstructed into TIF image slices. The resulting images, utilizing a 10X lens, had $0.9 \mu\text{m}$ voxel resolution. Scans were done for 10 min to cover one 2-mm-long section of the mid-leaf vasculature, using scan settings and lenses optimized for plant material (Earles et al., 2016).

MicroCT scans were analyzed using ImageJ to locate and count embolized cells over the entire 2-mm-long scanned leaf section. We quantified transfusion tracheid collapse by comparing transfusion tissue (TT) area of each experimental class using the mean of 3–8 clear cross-sectional slices per leaf scan, considering the hydrated class as the control representing pre-drought conditions. There was almost no variation within-leaf at the scale measured (nearest 0.0001 mm^2), and in fact many area measurements were identical. The TT was easily distinguishable from mesophyll because the greater relative density of their cell walls made tracheids appear brighter than surrounding living cells. We quantified transfusion tracheid collapse by comparing TT areas of hydrated leaves to those of bench-dried

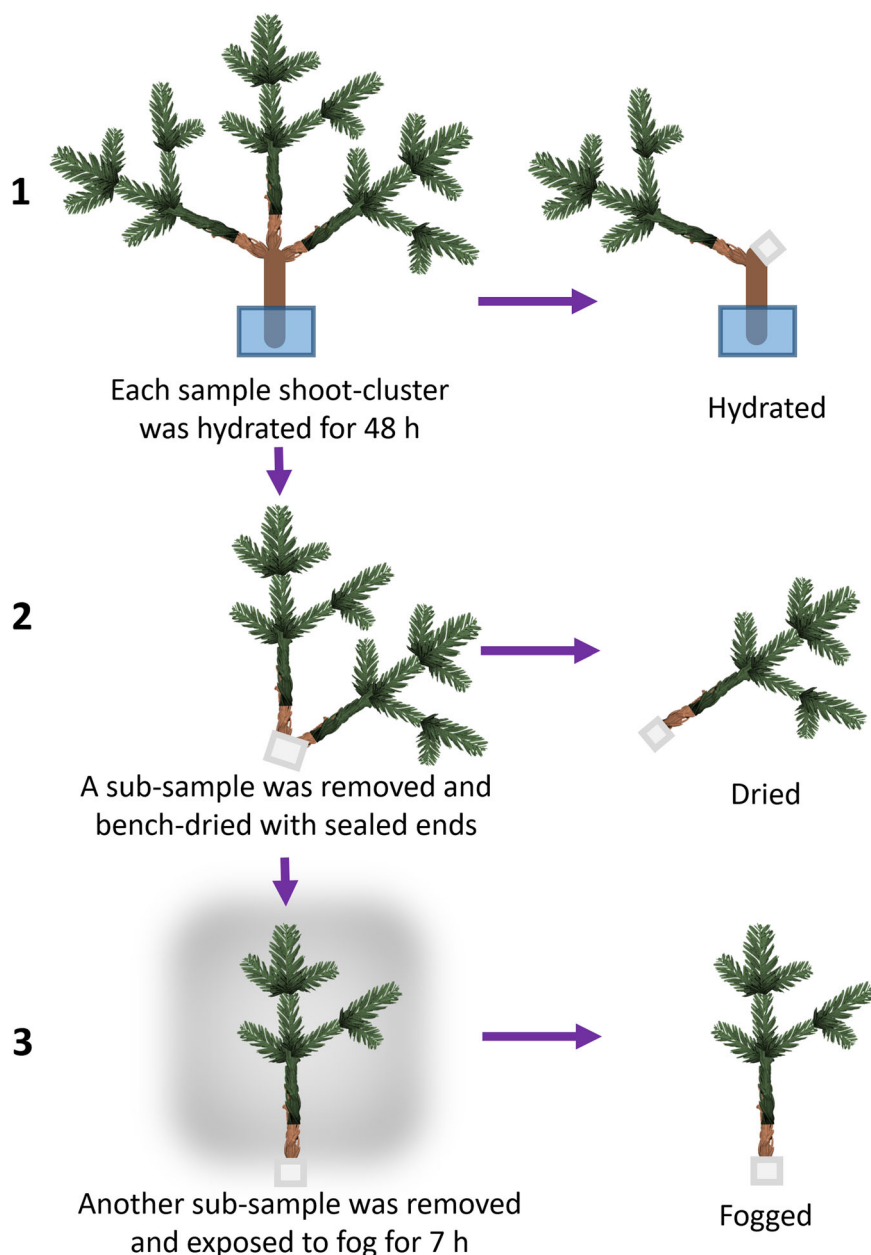


FIGURE 2 Experimental design. All 10 shoot-cluster samples were quickly recut under water after harvesting and allowed to fully hydrate (Step 1). A large subsample was removed from each for further treatment, leaving a smaller subsample (approximately one-third of the shoot-cluster) in water as the Hydrated treatment ($N = 10$). The removed subsamples, with paraffin-sealed cut-ends, were then bench-dried to their estimated turgor loss points (Step 2). Following bench-drying, a subsample from each of the 10 dried shoot-clusters (approximately one half) was retained as the Dried treatment ($N = 10$) and placed in a plastic bag to prevent further water loss. Finally, subsamples of 5 of the 10 bench-dried shoot-clusters, also with paraffin-sealed ends, were exposed to fog (Step 3) to form the Fogged treatment ($N = 5$). [Color figure can be viewed at wileyonlinelibrary.com]

leaves (buckling fraction = (hydrated TT area - droughted TT area) / hydrated TT area). Volumes of water released during tracheid buckling were computed by subtracting estimated TT volume of the dried class from that of the hydrated class (estimated TT volume = TT area \times (leaf length \times 0.95)). Differences in transfusion tissue cross-sectional area among hydrated, dried, and fogged classes were evaluated with mixed-effects analysis of covariance (ANCOVA) and compared using estimated marginal means for each treatment because of their suitability for unbalanced designs (Table 1). We included both tree and shoot cluster (nested within tree) as random effects on the model intercept, with treatment and sample height as fixed effects (formula: TT area \sim treatment + sample height + (1 | tree) + (1 | tree:cluster)). Both F statistics and p values were estimated using Satterthwaite's method of approximation. These analyses were implemented in the R packages lme4, lmerTest, and emmeans.

2.2 | Calculation of increased transpiration (ΔE) sustained by transfusion tracheid buckling

Following the drought-and-recovery experiment, we scaled up the information obtained on tracheid buckling in leaves to its tree-level significance by bringing together existing data on leaf anatomy, stomatal conductance, and microclimate of five tall (>109 m) individual *Sequoia* trees growing in Humboldt Redwoods State Park (hereafter HRSP-5 trees). To estimate the duration of increased transpiration that could be sustained by water released during tracheid buckling, we combined experimentally determined transfusion tissue buckling fraction (this study) with analyses of previously collected stomatal conductance (g_s , Mullin et al., 2009), leaf anatomy (Oldham et al., 2010), and tree-top micro-meteorological data from the HRSP-5 trees along with another set of identically collected micro

climate data from throughout the crowns of six additional *Sequoia* trees in HRSP, Prairie Creek Redwoods State Park, and Jedediah Smith Redwoods State Park (two trees per site, Sillett & Van Pelt, 2007). The HRSP-5 data set originated from a series of companion studies (Ambrose et al., 2010; Mullin et al., 2009; Oldham et al., 2010), which have not been analyzed collectively before, and we use unpublished data from these studies as described in the following paragraphs. It seems possible that mesophyll cells may also release water adding to the volume released during dehydration, but we did not observe any obvious change in mesophyll cell shape or size within the range of applied water stress, unlike the clear buckling of transfusion tracheids.

2.2.1 | Anatomy

We combined previously published data on TT cross-sectional areas (from HRSP-5 trees; Oldham et al., 2010) with leaf length and area data for the same samples. Shoots used for this structural analysis were collected across the crown depth from five trees. Height-paired inner and outer crown samples were taken from 26 heights, along with five treetop samples, and fully hydrated before preservation or scanning ($N = 57$ samples, each of which is the mean value of two replicate leaves, see anatomical methods in Oldham et al., 2010). After verifying through additional longitudinal leaf sectioning (for this study) that TT as a tissue does not taper along leaf length and extends nearly to the tip, we estimated its volume by multiplying mean TT cross-sectional area (highlighted in Figure 1a) by 95% of total leaf length. We estimated the hydraulic capacity of TT (mol m^{-2}) by converting volume to moles and dividing by leaf area. Potential quantities of water released by transfusion tracheid buckling in each sample were then estimated by multiplying the area-based molar quantity of water in the leaf's transfusion tissue by the buckling fraction estimated from the linear relationship between sample height and buckling among the nine tall samples. To explore other potential buckling scenarios, we also multiplied the minimum and maximum buckling fractions we observed by the molar quantities of water held in transfusion tissue.

2.2.2 | Stomatal conductance

Using fully hydrated shoots collected from upper, middle, and lower crowns of the HRSP-5 trees ($N = 15$ positions, each with two replicate cuttings), maximum stomatal conductance ($g_{s\text{max}}$) was measured under idealized conditions using light response curves from a LiCor 6400 portable photosynthesis system with a 2×3 cm standard leaf chamber equipped with a red-blue LED source (model 6400-02B; summary data published in Mullin et al., 2009). Curves were made with block temperature set to 25°C , reference CO_2 set to 400 ppm, leaf-to-air VPD maintained between 1.4 and 2.0 kPa, and the following photosynthetically active radiation ($\mu\text{mol m}^{-2} \text{s}^{-1}$) sequence: 2000, 1600, 1200, 900, 600, 400, 300, 200, 100, 50, 25, and 0. For the present study, we used the individual points

summarized in height-bins in Mullin et al. (2009) to develop a linear equation for the approximation of $g_{s\text{max}}$ from sample collection height, envisioning a worst-case (max observed ΔVPD at $g_{s\text{max}}$) response to a sudden VPD change per anatomical sample.

2.2.3 | Micrometeorological measurements

Treetop solar-powered micro-meteorological stations were deployed in the HRSP-5 trees to log temperature, relative humidity, leaf wetness, and other climatic variables every half-hour over the course of September 2007–September 2008 ($N = 5$ sensors, with a total of 21,000 half-hour measurement increments). We merged these records by time and day of the year with corresponding data from upper, middle, and lower crowns (centered by individual crown-depth) in six tall *Sequoia* trees from HRSP and two other primary forests (map of sensor locations within crowns and some totals published in Sillett & Van Pelt, 2007; $N = 21$ sensors, with 17,255 measurement increments in 2006–2007). We used data from all 26 sensors to calculate VPD from temperature and relative humidity (Nobel, 1983) to understand its maximum and typical values in relation to crown position. Because we were particularly interested in rapid in situ fluctuations in evaporative demand, we calculated the intensity of local VPD increase (ΔVPD) for each sensor as the differences between sequential VPD measurements over half-hour time increments. All peak values from individual sensors occurred in the summertime (June–August).

2.2.4 | Calculation of transpiration sustained

We estimated the seconds of transpiration sustained solely by water released during TT buckling (temporal reserves) in two steps. First, we computed the increased transpiration rate (ΔE , $\text{mol m}^{-2} \text{s}^{-1}$) for a given combination of stomatal conductance (g_s) and ΔVPD via the following equation (based on Nobel, 1983):

$$\Delta E = g_s \frac{\Delta\text{VPD}}{99.6},$$

where 99.6 is the barometric constant for the Bull Creek alluvial forest in Humboldt Redwoods State Park. Second, we computed local temporal reserves (in seconds) by dividing estimated ΔE by the molar quantity of water released per unit leaf area during tracheid collapse (mol m^{-2}). This calculation was based on the buckling fraction estimated from sample height (buckling fraction = $-97.584 \times \text{height} + 110.05$, $R^2 = 0.60$, $F = 10.56$, $p = 0.014$, $N = 9$ tall samples) multiplied by area-based transfusion tissue capacity (calculated from HRSP-5 anatomy data) as follows:

$$\begin{aligned} &\text{temporal reserves(s)} \\ &= \frac{\Delta E (\text{mol m}^{-2} \text{s}^{-1})}{\text{transfusion tissue capacity} (\text{mol m}^{-2}) \times \text{buckling fraction}} \end{aligned}$$

Available temporal reserves throughout the crown were assessed during a "worst case event" of maximum observed treetop ΔVPD

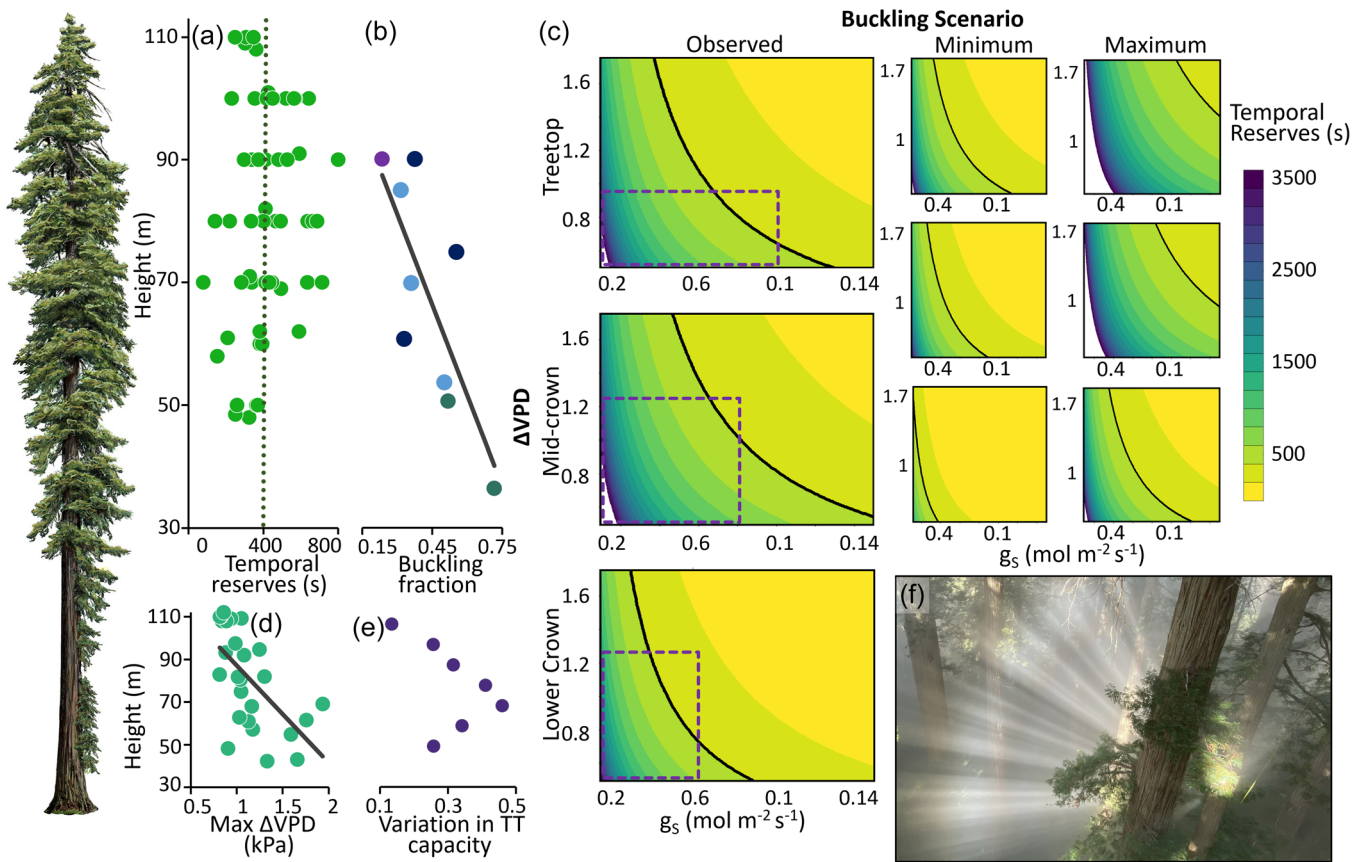


FIGURE 3 Leaf structure and function is closely coordinated with local risk of sunflecks. (a) Number of seconds of transpiration sustained by transfusion tissue (TT) buckling, given “worst-case” where leaves operate at maximum stomatal conductance (g_{smax}) and experience maximum increase in vapor pressure deficit (ΔVPD). Under observed (height-decreasing) buckling scenario, predicted TT buckling can sustain > 400 s (dotted line) of worst-case ΔE for approximately half the crown. (b) Fraction of the TT that buckled decreased with sample height in our dry-down experiment ($R^2 = 0.60$, $p = 0.014$). Colors indicate individual trees. (c) Temporal reserves (seconds of ΔE sustained – color scale) provided by TT buckling are examined across full observed ranges of ΔVPD and stomatal conductance (g_s) as well as minimum (23%) and maximum (71%) buckling scenarios applied across all 3 height-bins (columns). Rows show predicted values for treetop (108–112 m), mid-crown (70–90 m) and lower crown (<60m) height bins. Black isolines mark 400 s presumably needed for stomatal closure (leaves are protected by TT in operational space to left of these lines). Dashed purple boxes, shown only in observed scenario, represent expected operational ranges per height bin, bounded by local means of g_{smax} and maximum ΔVPD . (d) Within-crown distribution of maximum VPD increases over half-hour increments reveals widely variable change and greater extremes below 80 m ($R^2 = 0.37$, $p = 0.001$). (e) Coefficients of variation (SD/mean) in TT capacity per unit leaf area in 10 m height-bins peaks at 70 m, and is lowest at treetop, similar to peak variability in ΔVPD . (f) Sunflecks rapidly increase light availability in deeply-shaded lower crowns, they are a likely source of sudden VPD increases in this system. Tree illustration on left provided by Robert Van Pelt. [Color figure can be viewed at wileyonlinelibrary.com]

events occurring at locally estimated g_{smax} (see Figure 3a). As reported above, equations for estimating buckling fraction and g_{smax} from height were based on small datasets due to sampling constraints and limited access to microCT beamtime. They are thus limited in predictive power. To avoid over-reliance on these trends, we assessed the implications of minimum, maximum, and predicted buckling fraction across the full range of operational conditions under which tracheids might buckle. To find the range of protection offered by the three tracheid buckling scenarios, we calculated temporal reserves for all observed combinations of g_s and ΔVPD using our maximum observed values (peak g_{smax} and ΔVPD across all samples)

as limits to the potential ΔE space. Height-bin averages (local means of g_{smax} and max ΔVPD) defined the “expected operational range” within the full transpirational space (see Figure 3c). Following previous studies demonstrating far greater physiological (Mullin et al., 2009) and anatomical (Oldham et al., 2010) variation within crowns of tall trees than among them, we used shoot clusters as the sample unit rather than individual trees, but accounted for this in our use of mixed-effects ANCOVA to compare treatments. All data analyses, including matrix operations describing the range of potential conditions and exploratory surface plots (Figure 3), were done in the R statistical environment.

TABLE 2 Mixed-effect ANCOVA results

ANCOVA Results							Estimated marginal means		
	Sum Sq	Mean Sq	Num d.f.	Den d.f.	F	p value	Treatment	EM mean	SE
Treatment	0.00024	0.00012	2	12.81	25.43370	0.00003	Hydrated	0.01544	0.00156
Sample height	0.00005	0.00005	1	10.355	9.83620	0.01015	Dried	0.00838	0.0016
							Fog Exposed	0.01352	0.00179

Note: Treatment and sample height had significant effects on transfusion tissue area. Both tree and shoot cluster were included as random effects in the underlying linear model. Estimated marginal means of transfusion tissue area within each class are provided due to their usefulness for comparison of treatments with uneven sample sizes.

Abbreviations: ANCOVA, analysis of covariance; d.f., degree of freedom; SE, standard of error.

3 | RESULTS

Experimentally bench-dried leaves had smaller transfusion tissue cross-sectional areas than did the fully-hydrated control leaves (ANCOVA: $F = 25.43370$, p value = 0.00003; Figure 1b,c, Table 2), which we interpreted as buckling. Transfusion tissue buckling fraction decreased with height (reported in Methods, Figure 3b – excludes 2-m sample from UCD campus), ranging from a maximum reduction in area of 71% (at 37 m) to a minimum of 23% (at 90 m) after drying to within 0.1 MPa of the expected turgor loss point (Ishii et al., 2014). Assuming, as we observed, consistent buckling along the leaf length, then the fractional reduction in transfusion tissue cross-sectional area (buckling fraction) is equal to the fractional decrease in its volume. Fogging restored transfusion tissue area to approximately its full pre-drought level (Figure 1c, Table 2). Both the water-holding capacity of transfusion tissue per unit leaf area ($N = 57$, $R^2 = 0.44$, $F = 41.6$, $p < 0.0001$) and maximum stomatal conductance (g_{smax}) under idealized conditions increased with height ($N = 14$, $R^2 = 0.35$, $F = 6.40$, $p = 0.026$). Over the half-hour increments measured, the maximum single VPD increase (ΔVPD) in any individual treetop was +0.96 kPa, while below 90 m the max ΔVPD was +1.9 kPa (Figure 2d). Levels of relative humidity suggest that wet air (determined here as $\geq 90\%$ RH) was present during 63% of summer hours between midnight and 06:00. Treetop leaf wetness was detected at 05:30 on 55% of summer mornings and was typically maintained until ~11:30. We found a greater ΔVPD (linear height trend $N = 26$, $R^2 = 0.37$, $F = 14.0$, $p = 0.001$) and variability in lower and middle crowns (< 90 m, $F = 0.140$, d.f._{up} = 10, d.f._{low} = 14, $p = 0.004$, $SD = 0.344$, $\bar{x}^- = 1.25$ kPa) than in the upper crown ($SD = 0.126$, $\bar{x}^- = 0.94$ kPa). All maximum ΔVPD events occurred between the afternoon hours of 13:00–15:00, when leaf surfaces were dry.

The observed height-decreasing buckling scenario estimated that amount of water released per m² of leaf area during buckling peaked at approximately 70 m above ground. Under the crown-wide minimum and maximum buckling scenarios, released water followed patterns of transfusion tissue capacity (Figure 3a,c). Within the expected operational range (bounded by local means of ΔVPD and g_{smax}), transfusion tissue buckling sustained ΔE up to 400 s, presumably long enough for stomatal closure (based on the closely related *Metasequoia*), under nearly all conditions. While this assumes stomata behave as predicted, the estimated volume of water released

was consistent with approximately 400 s duration (Figure 3c). Using the range of observed buckling fractions, and assuming a “worst case” where the maximum observed ΔVPD events coincided with full stomatal openness (i.e., at g_{smax}), we found that the minimum observed buckling fraction (23%) would be insufficient to support ΔE at most heights, unless lower and mid-crown leaves were operating well below either maximum or reported in situ g_s (Ambrose et al., 2010; Figure 3c). On the other hand, under this same worst-case, when applying the maximum observed buckling fraction (71%) to the entire crown, we estimated potentially excessive water release with the full hydraulic demand of ΔE sustained > 400 s at all heights, and above 70 m quantities released were up to eight times more than required transpirational reserves (Figure 3c).

Drought treatments produced embolisms in some transfusion and xylem tracheids. While at all eight sample heights $< 0.05\%$ tracheids were air-filled in hydrated leaves, 4 of 10 experimentally-dried samples had embolisms in the range of 1%–15% of tracheids. The remaining six bench-dried samples had an embolism frequency similar to hydrated leaves. In the four samples that experienced cavitation, the outermost row of xylem was air-filled only in leaves from 37 to 51 m with patchy embolisms among transfusion tracheids. In all cases, exposure to fog reduced embolism frequency to levels indistinguishable from the hydrated leaves, though dried leaves did exhibit more frequent embolisms (1%–15% of tracheids were embolized, $N = 4$, one-sided Fisher's exact $p = 0.014$).

4 | DISCUSSION

The depth of tall *Sequoia* crowns creates steep gradients in light, temperature, and relative humidity with microclimates ranging from relatively stable at the treetop to highly variable in the mid-crown. Structural and physiological plasticity of *Sequoia* leaves appear to support leaf survival in the face of environmental perturbations such as the arrival of sunflecks that can induce VPD changes of the magnitude we observed within tall *Sequoia* crowns. We observed transfusion tracheid buckling during water stress under laboratory conditions, and estimated volumes of water released appear to be in synchrony with our measurement of in situ environmental variability. Our calculations predict that within the expected operation range, tracheid buckling almost always provides adequate water to allow

approximately 400 s of supplemental transpiration throughout the crown (Figure 3b,c). In comparison to fully hydrated leaves, tracheid buckling induced by experimental bench-drying reduces the transfusion tissue cross-sectional area by 23%–71% (X-ray microCT images of dried samples; Figure 1b,c) with the fraction of buckling transfusion tracheids decreasing with increasing height in the crown (Figure 2b). A height-associated decrease in buckling contrasts with results from *Cryptomeria japonica*, where tracheid buckling increases with height (Azuma et al., 2016). Deeper crowns of much taller *Sequoia* may require a balance between buckling and transfusion tissue area that supports more intense microclimatic variation in their shady depths. Compared with consistently bright treetops, we observed nearly double the intensity of ΔVPD in lower and mid-crown environments (<90 m). There is also greater local variability in ΔVPD below 90 m with the highest intensity and broadest variation ΔVPD events occurring at 70 m, where transfusion tissue capacity to release water is also most variable (Figure 3a–e). Under our experimental conditions, foliar absorption of water restores transfusion tissue to its pre-drought volume (Figure 1c). Our sensors detected sustained leaf-wetness events in tall *Sequoia* crowns on most summer (June–August) mornings, suggesting that leaves have regular access to aerial water sources. Tracheid buckling may provide protection from rising tension by halting its increase in proximal tissues at the buckling threshold, representing a stop-point for tension that isolates risk in the leaf hydraulic segment (Zhang et al., 2016). We picture this stop-point as the level of tension that induces enough hydraulic separation of leaf and shoot, through tracheid buckling or cavitation, to protect the shoot should tension continue to rise in the leaf. Such a stop-point is especially important where, as we observed in *Sequoia*, the buckling threshold is below the level of tension (at less negative pressure) that results in widespread cavitation of water transport tissue.

As we show here, water crossing the surface of *Sequoia* leaves can remove buckling. It seems reasonable that this process also occurs under natural conditions. Predawn Ψ exceeding the gravitational potential gradient has been observed following natural leaf-wetting in both tall *Sequoia* and *Picea sitchensis* (Jennings, 2002; Kerhoulas et al., 2020), and sap-flow reversal has been observed in *Sequoia* (Burgess & Dawson, 2004). Even if high tension due to height is permanent in the trunk, local hydraulic segmentation due to resistance between leaf and stem, or at other junctures (Johnson et al., 2016; Tyree, 1988; Zimmermann, 1978), might permit recovery in the leaf. In addition to typical levels of hydraulic segmentation (Zimmermann, 1978), the buckling of tracheids should disrupt hydraulic conductivity between leaf and stem (Bucci et al., 2003; Hochberg et al., 2017; Zhang et al., 2016). Pending repair of this impediment to flow, we envision high resistance functionally isolating the leaf, causing an accumulation of water that allows leaf-level Ψ to increase until recovery thresholds are met—and water exchange with the stem can resume. By slowing water export from the leaf (Zhang et al., 2014), transfusion tracheid buckling may promote localized Ψ increases that facilitate embolism repair in tall trees after leaf wetting—an area worthy of future research. In other conifers, such as

Douglas-fir (*Pseudotsuga menziesii*), regular cycles of leaf-level embolism and repair appear to be part of their hydraulic strategy (Johnson et al., 2012; Woodruff et al., 2007). Douglas-fir, which can approach 100-m tall may be a good candidate for recovery via foliar water absorption because approximately 40% of its leaf surface area is covered in algae, presumably enhancing leaf wetness (Chin & Sillett, 2019).

The presence of regular tracheid buckling cycles could provide insight into *Sequoia* leaf longevity. It appears that damage accumulation is sufficiently low to allow a multi-year leaf lifespan, although both buckling and embolism fatigue warrant further investigation. Regular and sustained summertime leaf wetness, as during summer (June–August) 2008 when our treetop leaf-wetness sensors were in place, may allow tall *Sequoias* to rely on transfusion tissue to provide a hydraulic buffer against rapid fluctuations in microclimate. *Sequoia* possesses axial leaves specialized nonphotosynthetic leaf type capable of triple the water absorption rate of the much more abundant peripheral leaves. Axial leaves have more than twice the transfusion tissue area of peripheral leaves and occur only along central woody shoots, likely enhancing their survival and pointing toward a link between transfusion tissue water release capacity and foliar water uptake (Chin et al., 2022). Maximum variability in peripheral-leaf transfusion tissue investment and peak seconds of ΔE sustained occur in the middle crown at approximately 70 m (Figure 3a,c,e). At and below the mid-crown zone, morphology of *Sequoia* foliage is related to light availability, but light acclimation disappears in the upper crown (Ishii et al., 2008). The mid-crown is the zone with both maximum intensity and variability of ΔVPD as well as concentration of crown structures such as limbs and trunk reiterations. (Sillett & Van Pelt, 2007; Figure 3d,e). Complex mid-crown structure combined with high leaf area may create patchy light environments that increase local variability brought on by sunflecks (Figure 3f), contributing to inconsistency in requirements for transfusion tissue capacity.

Does tracheid buckling alone provide adequate water supply to allow time for stomatal closure if no additional water is available from the stem? While we are unlikely to have uncovered the full range of minimum and maximum buckling fractions within *Sequoia* crowns, water release under a scenario of crown-wide minimum buckling would not adequately protect the lower two-thirds of the tree (Figure 3c). However, if the maximum buckling fraction is applied to the entire crown, treetops could release eight-times more water than required to allow stomatal closure (Figure 3c). Our measurements suggest the height-decreasing buckling fraction we observe is optimal and can, under most combinations of g_s and ΔVPD , sustain ΔE for a minimum of 400 s, which is the approximate time reserve necessary for stomatal closure (Martins et al., 2016; McAdam & Brodribb, 2014; Figure 3c). Although the behavior of stomata during our experiment and within-crown variation in closure rates in *Sequoia* are unknown, we find the closeness of our estimated values to this 400 s time to be suggestive of coordination between hydraulic risk and transfusion tracheid buckling (Figure 3c). When approaching g_{smax} , leaves may be insufficiently protected by transfusion tracheid buckling when

maximum levels of ΔVPD are experienced due to sudden temperature changes brought on by sunflecks and other events (Schymanski et al., 2013; Figure 3a,c,f). However, this “worst case” is very unlikely to be realized, because extreme ΔVPD events occur during summertime (June–August) afternoons, when g_s is far below its maximum (Ambrose et al., 2010). In the same approximately 110-m-tall individual trees, in situ measurement of sapflow suggest that mean summertime g_s in the treetops was roughly one-quarter of mean g_{smax} ($\sim 0.023 \text{ mol m}^{-2} \text{ s}^{-1}$ in summer; Ambrose et al., 2010). The area-based capacity of transfusion tissue is greatest at approximately 90 m, and estimated temporal reserves for treetop samples (108–112 m) decrease from peak mid-crown values and coalesce to a strikingly consistent range (Figure 3a). This treetop consistency in temporal reserves is driven by the loss of among-tree variability in transfusion tissue capacity, perhaps suggesting that structural limits are being approached (Figure 3a,e). Indeed, trees near *Sequoia*'s northern and southern range limits reach similar levels of maximum transfusion tissue area at different heights, a possible explanation for why approximately 80-m-tall southern trees have similar foliar hydraulic capacity to approximately 110-m-tall northern trees (Ishii et al., 2014). Treetop leaves of *Sequoia* may not require as much capacity to release water as elsewhere in the crown, because they exist in the least variable environment (Figure 3d), are closely appressed to succulent shoots, and have smaller stomata that may be capable of faster closure (Chin & Sillett, 2019; Drake et al., 2013; Ishii et al., 2014). Treetop leaves also have the widest variability in transfusion tracheid diameter and circularity (Oldham et al., 2010), raising the possibility of a series of buckling thresholds at greater tensions than we induced.

Our analyses necessitate further consideration of the limits to maximum tree height, which include hydraulic limitation and phloem transport capacity (Jensen & Zwieniecki, 2013; Koch et al., 2004; Ryan & Yoder, 1997). Among the requirements for heights >30m—trees presumably too tall to refill embolisms from root-sourced water—may be adequate foliar absorption capacity and an abiotic dimension related to presence of water on leaf surfaces. Although recovery due to foliar absorption is crown-wide, transfusion tissue investment and the ability of tracheids to buckle could be approaching their limits in the tops of the tallest *Sequoia* (Figure 3a,b). A release-refill strategy may become untenable in trees much taller than those examined here, where treetop variability in transfusion tissue capacity already becomes tightly constrained (Figure 2e). The fraction of transfusion tissue that releases water may be limited by inflexibility of the extremely dense mesophyll seen near the tops of tall *Sequoia* (Mullin et al., 2009; Oldham et al., 2010). This potential structural limitation to buckling fraction may force the prioritization of transfusion tissue at the expense of photosynthetic mesophyll.

In conclusion, the amount of water released during tracheid buckling can accommodate increased evapotranspiration resulting from sudden changes in ΔVPD , sustaining approximately 400 s of transpiration throughout *Sequoia* crowns. In addition, tracheid buckling can provide a stop point for translation of tension below the cavitation threshold even though minor cavitation occurs.

Observations of buckling recovery from foliar water uptake indicate the capacity to sustain multiple stress events to promote leaf survival in this evergreen species. With their pattern of investment in transfusion tissue, *Sequoia* has an optimized temporal reserve system to protect leaves across a wide operational range (Figure 3c). Deep crowns of tall *Sequoia* are supported by a finely tuned coupling of leaf vascular anatomy and stomatal conductance with microclimatic variability – a strategy that may depend on foliar water absorption.

ACKNOWLEDGMENTS

We are thankful to B. Chin for assistance with the experiment, R. Van Pelt for providing the tree illustration in Figure 2, Z. Moore for preparing the cross-section in Figure 1a, and W. Azuma and the anonymous reviewers for useful comments on the manuscript. J. Heimer of the statistical consulting service at ETH-Zurich was very helpful in planning the analysis of our experimental data. We also thank D. Parkinson and H. Barnard at the LBNL Advanced Light Source, beamline 8.3.2, for their assistance with the tomography. Alana R.O. Chin is very grateful to A.M.F. Tomescu for many years of discussion of tracheid buckling, she was supported by a Graduate Research Fellowship from NSF, Paula Guzmán-Delgado was supported by a Katherine Esau Fellowship from UC Davis. Open access funding provided by Eidgenössische Technische Hochschule Zurich. Open access funding provided by Eidgenössische Technische Hochschule Zurich.

DATA AVAILABILITY STATEMENT

The data that support the findings of this study are openly available at <https://doi.org/10.13140/RG.2.2.32685.77288>.

ORCID

Alana R. O. Chin  <http://orcid.org/0000-0002-3862-9563>

Paula Guzmán-Delgado  <http://orcid.org/0000-0002-5264-2430>

Andrew R. McElrone  <http://orcid.org/0000-0001-9466-4761>

REFERENCES

- Ambrose, A.R., Sillett, S.C., Koch, G.W., Van Pelt, R., Antoine, M.E. & Dawson, T.E. (2010) Effects of height on treetop transpiration and stomatal conductance in coast redwood (*Sequoia sempervirens*). *Tree Physiology*, 30, 1260–1272.
- Azuma, W., Ishii, H.R., Kuroda, K. & Kuroda, K. (2016) Function and structure of leaves contributing to increasing water storage with height in the tallest *Cryptomeria japonica* trees of Japan. *Trees*, 30, 141–152.
- Bannister, P. (1986) Drought resistance, water potential and water content in some New Zealand plants. *Flora*, 178, 23–40.
- Brodersen, C. & McElrone, A. (2013) Maintenance of xylem network transport capacity: a review of embolism repair in vascular plants. *Frontiers of Plant Science*, 4, 108.
- Brodribb, T.J. & Holbrook, N.M. (2005) Water stress deforms tracheids peripheral to the leaf vein of a tropical conifer. *Plant Physiology*, 137, 1139–1146.
- Burgess, S.S.O. & Dawson, T. (2004) The contribution of fog to the water relations of *Sequoia sempervirens*: foliar uptake and prevention of dehydration. *Plant, Cell & Environment*, 27, 1023–1034.
- Chin, A.R., Guzmán-Delgado, P., Sillett, S.C., Orozco, J., Kramer, R.D., Kerhoulas, L.P. et al. (2022) Shoot dimorphism enables *Sequoia sempervirens* to separate requirements for foliar water uptake and photosynthesis. *American Journal of Botany*, 109(4), 564–579.

- Chin, A.R. & Sillett, S.C. (2016) Phenotypic plasticity of leaves enhances water-stress tolerance and promotes hydraulic conductivity in a tall conifer. *American Journal of Botany*, 103, 796–807.
- Chin, A.R. & Sillett, S.C. (2019) Within-crown plasticity in leaf traits among the tallest conifers. *American Journal of Botany*, 106, 174–186.
- Drake, P.L., Froend, R.H. & Franks, P.J. (2013) Smaller, faster stomata: scaling of stomatal size, rate of response, and stomatal conductance. *Journal of Experimental Botany*, 64, 495–505.
- Earles, J.M., Sperling, O., Silva, L.C., McElrone, A.J., Brodersen, C.R. & North, M.P. et al. (2016) Bark water uptake promotes localized hydraulic recovery in coastal redwood crown. *Plant, Cell & Environment*, 39, 320–328.
- Esau, K. (1977) *Anatomy of seed plants*. New York, NY: John Wiley & Sons. Inc.
- Guzmán-Delgado, P., Earles, M.J. & Zwieniecki, M.A. (2018) Insight into the physiological role of water absorption via the leaf surface from a rehydration kinetics perspective. *Plant, Cell & Environment*, 41, 1886–1894.
- Hochberg, U., Windt, C.W., Ponomarenko, A., Zhang, Y.J., Gersony, J., Rockwell, F.E. et al. (2017) Stomatal closure, basal leaf embolism, and shedding protect the hydraulic integrity of grape stems. *Plant Physiology*, 174, 764–775.
- Ishii, H.R., Azuma, W., Kuroda, K. & Sillett, S.C. (2014) Pushing the limits to tree height: could foliar water storage compensate for hydraulic constraints in *Sequoia sempervirens*? *Functional Ecology*, 28, 1087–1093.
- Ishii, H.T., Jennings, G.M., Sillett, S.C. & Koch, G.W. (2008) Hydrostatic constraints on morphological exploitation of light in tall sequoia *sempervirens* trees. *Oecologia*, 156, 751–763.
- Jennings, G.M. (2002) Vertical hydraulic gradients and the cause of foliar variation in tall redwood trees (*Sequoia sempervirens*), Masters thesis. Humboldt State University.
- Jensen, K.H. & Zwieniecki, M.A. (2013) Physical limits to leaf size in tall trees. *Physical Review Letters*, 110, 018104.
- Johnson, D.M., McCulloh, K.A., Woodruff, D.R. & Meinzer, F.C. (2012) Hydraulic safety margins and embolism reversal in stems and leaves: why are conifers and angiosperms so different? *Plant Science*, 195, 48–53.
- Johnson, D.M., Wortemann, R., McCulloh, K.A., Jordan-Meille, L., Ward, E., Warren, J.M. et al. (2016) A test of the hydraulic vulnerability segmentation hypothesis in angiosperm and conifer tree species. *Tree Physiology*, 36, 983–993.
- Kerhoulas, L.P., Weisgrau, A.S., Hoefft, E.C. & Kerhoulas, N.J. (2020) Vertical gradients in foliar physiology of tall *Picea sitchensis* trees. *Tree Physiology*, 40, 321–332.
- Koch, G.W., Sillett, S.C., Jennings, G.M. & Davis, S.D. (2004) The limits to tree height. *Nature*, 428, 851–854.
- Martins, S.C., McAdam, S.A., Deans, R.M., DaMatta, F.M. & Brodribb, T.J. (2016) Stomatal dynamics are limited by leaf hydraulics in ferns and conifers: results from simultaneous measurements of liquid and vapor fluxes in leaves. *Plant, Cell & Environment*, 39, 694–705.
- McAdam, S.A. & Brodribb, T.J. (2014) Separating active and passive influences on stomatal control of transpiration. *Plant Physiology*, 164, 1578–1586.
- Mullin, L.P., Sillett, S.C., Koch, G.W., Tu, K.P. & Antoine, M.E. (2009) Physiological consequences of height-related morphological variation in *Sequoia sempervirens* foliage. *Tree Physiology*, 29, 999–1010.
- Nobel, P.S. (1983) *Biophysical plant physiology and ecology*. San Francisco, CA: W H Freeman and company.
- Oldham, A.R., Sillett, S.C., Tomescu, A.M. & Koch, G.W. (2010) The hydrostatic gradient, not light availability, drives height-related variation in *Sequoia sempervirens* (cupressaceae) leaf anatomy. *American Journal of Botany*, 97, 1087–1097.
- Parker, J. (1952) Desiccation in conifer leaves: anatomical changes and determination of the lethal level. *Bot. Gazette*, 114, 189–198.
- Petruzzellis, F., Pagliarani, C., Savi, T., Losso, A., Cavalletto, S. & Tromba, G. et al. (2018) The pitfalls of in vivo imaging techniques: evidence for cellular damage caused by synchrotron x-ray computed micro-tomography. *New Phytologist*, 220, 104–110.
- Ryan, M.G. & Yoder, B.J. (1997) Hydraulic limits to tree height and tree growth. *Bioscience*, 47, 235–242.
- Schreel, J.D.M. & Steppe, K. (2020) Foliar water uptake in trees: negligible or necessary? *Trends in Plant Science*, 25, 590–603.
- Schymanski, S.J., Or, D. & Zwieniecki, M. (2013) Stomatal control and leaf thermal and hydraulic capacitances under rapid environmental fluctuations. *PLoS One*, 8, e54231.
- Sillett, S.C. & Van Pelt, R. (2007) Trunk reiteration promotes epiphytes and water storage in an old-growth redwood forest canopy. *Ecological Monographs*, 77, 335–359.
- Tyree, M.T. (1988) A dynamic model for water flow in a single tree: evidence that models must account for hydraulic architecture. *Tree Physiology*, 4, 195–217.
- Tyree, M.T. & Sperry, J.S. (1989) Vulnerability of xylem to cavitation and embolism. *Annual Review of Plant Biology*, 40, 19–36.
- Woodruff, D.R., McCulloh, K.A., Warren, J.M., Meinzer, F.C. & Lachenbruch, B. (2007) Impacts of tree height on leaf hydraulic architecture and stomatal control in Douglas-fir. *Plant Cell, & Environment*, 30, 559–569.
- Zhang, Y.J., Rockwell, F.E., Graham, A.C., Alexander, T. & Holbrook, N.M. (2016) Reversible leaf xylem collapse: a potential “circuit breaker” against cavitation. *Plant Physiology*, 172, 2261–2274.
- Zhang, Y.J., Rockwell, F.E., Wheeler, J.K. & Holbrook, N.M. (2014) Reversible deformation of transfusion tracheids in *Taxus baccata* is associated with a reversible decrease in leaf hydraulic conductance. *Plant Physiology*, 165, 1557–1565.
- Zimmermann, M.H. (1978) Hydraulic architecture of some diffuse-porous trees. *Canadian Journal of Botany*, 56, 2286–2295.

How to cite this article: Chin, A.R.O., Guzmán-Delgado, P., Sillett, S.C., Kerhoulas, L.P., Ambrose, A.R., McElrone, A.R., et al. (2022) Tracheid buckling buys time, foliar water uptake pays it back: Coordination of leaf structure and function in tall redwood trees. *Plant, Cell & Environment*, 1–10.
<https://doi.org/10.1111/pce.14381>